available at www.sciencedirect.com
journal homepage: www.eu-openscience.europeanurology.com

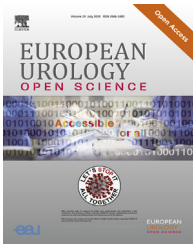

European Association of Urology

Bladder Cancer

Sexual Dimorphism in Outcomes of Non–muscle-invasive Bladder Cancer: A Role of CD163+ Macrophages, B cells, and PD-L1 Immune Checkpoint

Stephen Chenard [a,b,†], *Chelsea Jackson* [a,c,†], *Thiago Vidotto* [d], *Lina Chen* [c], *Céline Hardy* [a,c], *Tamara Jamaspishvilli* [a,c], *David Berman* [a,b,c], *D. Robert Siemens* [a,b,e], *Madhuri Koti* [a,b,e,*]

[a] *Queen's Cancer Research Institute, Kingston, ON, Canada;* [b] *Department of Biomedical and Molecular Sciences, Queen's University, Kingston, ON, Canada;* [c] *Department of Pathology and Molecular Medicine, Queen's University, Kingston, ON, Canada;* [d] *Department of Pathology, Johns Hopkins School of Medicine, Baltimore, MD, USA;* [e] *Department of Urology, Queen's University, Kingston, ON, Canada*

Article info

Article history:
Accepted May 13, 2021

Associate Editor:
Guillaume Ploussard

Keywords:
Non–muscle-invasive bladder cancer
Sexual dimorphism
Tumor immune microenvironment
Tumor-associated macrophages
B cells

Abstract

Background: Non–muscle-invasive bladder cancer (NMIBC) is over three times as common in men as it is in women; however, female patients do not respond as well to immunotherapeutic treatments and experience worse clinical outcomes than their male counterparts. Based on the established sexual dimorphism in mucosal immune responses, we hypothesized that the tumor immune microenvironment of bladder cancer differs between the sexes, and this may contribute to discrepancies in clinical outcomes.

Objective: To determine biological sex-associated differences in the expression of immune regulatory genes and spatial organization of immune cells in tumors from NMIBC patients.

Design, setting, and participants: Immune regulatory gene expression levels in tumors from male (n = 357) and female (n = 103) patients were measured using whole transcriptome profiles of tumors from the UROMOL cohort. Multiplexe immunofluorescence was performed to evaluate the density and spatial distribution of immune cells and immune checkpoints in tumors from an independent cohort of patients with NMIBC (n = 259 males and n = 73 females).

Outcome measurements and statistical analysis: Transcriptome sequencing data were analyzed using DESeq2 in R v4.0.1, followed by application of the Kruskal-Wallis test to determine gene expression differences between tumors from males and females. Immunofluorescence data analyses were conducted using R version 3.5.3. Survival analysis was performed using survminer packages.

Results and limitations: High-grade tumors from female patients exhibited significantly increased expression of B-cell recruitment (*CXCL13*) and function (*CD40*)-associated genes and the immune checkpoint genes *CTLA4*, *PDCD1*, *LAG3*, and

† These authors contributed equally.
* Corresponding author. Department of Biomedical and Molecular Sciences and Obstetrics and Gynecology, Queens University, Kingston, Ontario K7L3N6, Canada. Tel. +1 613 533 2979.
E-mail address: kotim@queensu.ca (M. Koti).

http://dx.doi.org/10.1016/j.euros.2021.05.002

ICOS. Tumors from female patients showed significantly higher infiltration of PD-L1 + cells and CD163+ M2-like macrophages than tumors from male patients. Increased abundance of CD163+ macrophages and CD79a+ B cells were associated with decreased recurrence-free survival.

Conclusions: These novel findings highlight the necessity of considering sexual dimorphism in the design of future immunotherapy trials in NMIBC.

Patient summary: In this study, we measured the abundance of various immune cell types between tumors from male and female patients with non–muscle-invasive bladder cancer. We demonstrate that tumors from female patients have a significantly higher abundance of immunosuppressive macrophages that express CD163. Higher abundance of tumor-associated CD163-expressing macrophages and B cells is associated with shorter recurrence-free survival in both male and female patients.

1. Introduction

Urothelial bladder cancer is the tenth most common cancer worldwide, with an estimated 549 000 incident cases and 200 000 deaths caused by the disease annually [1]. Bladder cancer can broadly be categorized based on the depth of tumor invasion. Approximately 75% of incident cases present as non–muscle-invasive bladder cancer (NMIBC), while the rest are classified as muscle-invasive disease [2]. The first-line treatment for bladder cancer is transurethral resection of bladder tumor (TURBT) surgery. Following surgical resection, patients with high-risk features (such as high stage, grade, or tumor multifocality) [3] are best treated with intravesical bacillus Calmette-Guérin (BCG) immunotherapy. BCG is a live-attenuated form of *Mycobacterium bovis*, and in addition to its clinical role in treating high-risk NMIBC, BCG is also used as a vaccine for the prevention of tuberculosis.

While the incidence of bladder cancer is over three times higher in men [1], women suffer earlier recurrences following treatment with BCG immunotherapy and experience shorter progression-free survival (PFS) when compared with their male counterparts [4–6]. Aligning with this, patient biological sex has recently emerged as an important factor in determining response to contemporary immunotherapies, such as anti-PD-1/PD-L1 and anti-CTLA4 immune checkpoint blockade therapy [7–9]. Clearly, patient sex (biological differences) and gender (social/behavioral differences) are associated with the incidence and clinical outcomes of NMIBC; however, these factors are understudied in biomarker and treatment design [10,11].

The pre-treatment tumor immune microenvironment (TIME) is a critical determinant of response to immunomodulation in several cancer types [12]. Emerging evidence suggests that the TIME plays a similarly important role in determining the response of bladder cancer patients to treatment with BCG immunotherapy [13,14]. Both host and cancer cell intrinsic factors influence the recruitment and functional states of immune cells, meaning the TIME of NMIBC can range across a spectrum from non-inflamed (low/no immune infiltration) to highly inflamed (high immune cell infiltration) [15].

Under normal physiological conditions, macrophages are the most abundant resident innate immune cells within the bladder mucosa [16]. Furthermore, preclinical studies in murine models have shown that females exhibit a higher magnitude of immune responses to urinary pathogens than males [17]. Advancing age, microbial challenges, host genetics, and postmenopausal hormonal changes also contribute to an increased recruitment of adaptive immune cell populations in the female bladder compared with that in males (unpublished data). Despite mounting evidence of the importance of these cell types in response to immunomodulatory therapy in several other cancers, their sex-specific roles and functional states within the NMIBC TIME have yet to be elucidated fully.

We hypothesized that the TIME of NMIBC would demonstrate significant differences between the sexes and, second, that this sexual dimorphism may be associated with clinical outcomes. To test this hypothesis, we utilized two large, independent cohorts of patients with NMIBC: the UROMOL cohort, a publicly available dataset of tumors from 460 patients [18], and the Kingston Health Sciences Center (KHSC) cohort (n = 332 patients). We evaluated the tumor transcriptome profiles of the UROMOL cohort to determine sex-associated differences in immune regulatory (with stimulatory and inhibitory functions) genes. Guided by the results of this gene expression analysis, we further investigated the density and spatial distribution of selected immune cell populations and immune checkpoint proteins in tumors from patients in the KHSC cohort. Findings from our study provide the first evidence for sex-associated differences in the TIME of NMIBC.

2. Patients and methods

2.1. Patient cohorts and clinical data

This study was approved by the Ethics Review Board at Queen's University. Clinical details of the UROMOL cohort were previously

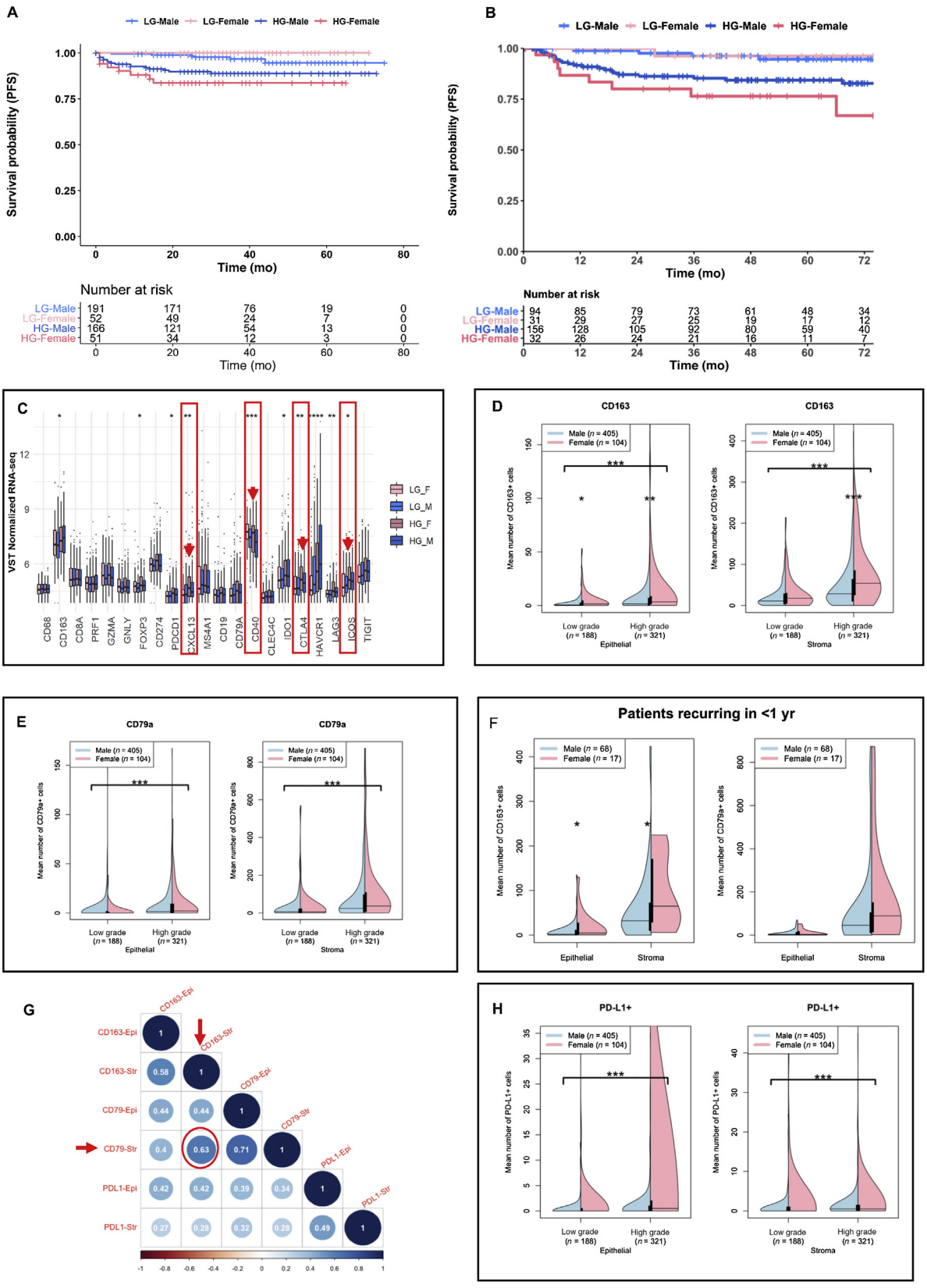

Fig. 1 – Patients with NMIBC exhibit sexual dimorphism in progression-free survival and tumor immune microenvironment. Kaplan-Meier survival curves showing female patients with high-grade NMIBC experienced significantly ($p < 0.001$) shorter PFS than their male counterparts and patients with low-grade tumors, in both (A) the UROMOL and (B) the KHSC cohorts. Kaplan-Meier survival analyses were performed using log-rank statistics with survival and survminer packages. (C) High-grade tumors from female patients in the UROMOL cohort exhibit significantly increased expression of immunoregulatory genes *CXCL13*, *PDCD1*, *CD40*, *CTLA4*, and *ICOS*. VST-normalized genes between four cohorts are as follows: high-grade cancer in females (HG_F), low-grade cancer in females (LG_F), high-grade cancer in males (HG_M), and low-grade cancer in males (LG_M). The Kruskal-Wallis test was employed to determine statistically significant differences. Violin plots of the mean cell counts for (D) CD163+ and (E) CD79a+ cell populations

reported by Hedegaard et al [18]. The KHSC cohort included 509 NMIBC archival TURBT surgeries from 332 patients between 2008 and 2016. Cases were reviewed by expert pathologists (D.B. and L.C.), using the World Health Organization 2016 grading system [19] and are described in Supplementary Table 1. Six tissue microarrays (TMAs) were constructed with duplicate 1.0-mm cores. Recurrence was defined as the time from each patient's earliest TURBT resection to next malignant diagnosis. Operative notes were reviewed to exclude re-resections as recurrences.

2.2. RNA-sequencing data analysis

Raw RNA-sequencing data from 460 NMIBC samples in the UROMOL cohort [18] were downloaded (https://www.ebi.ac.uk/ega/studies/EGAS00001001236), and VST-normalized data were obtained by employing the vst function on DESeq2 in R v4.0.1. Further, we compiled a list comprising immune-cell markers and regulatory genes (with stimulatory and inhibitory functions) based on our previous report [20]. We then compared the expression of these VST-normalized genes between four groups of patients: high-grade female, low-grade female, high-grade male, and low-grade male. The Kruskal-Wallis test was employed to determine significant differences between the four groups.

2.3. Multiplex immunofluorescence staining for immune markers

TMAs were stained with three panels of primary antibodies. The first panel contained antibodies against CD3+, CD8+, Ki67+, CK5+ and FoxP3+ cells. The second panel contained antibodies against PD-1+, PD-L1+, IDO-1+, and CK5+ cells. The third panel contained antibodies against CD163+, CD79a+, CD103+, and GATA3+ cells. Expression for the following cell types and immune checkpoints was evaluated in the epithelial and stromal compartments: T cells (CD3+CD8+Ki67, CD3+CD8+Ki67+, CD3+CD8-FOXP3–, and CD3+CD8-FOXP3+), immune checkpoints (PD-1+, PDL1+, and CK5+PDL1+), B cells (CD79a+), M2-like tumor-associated macrophages (TAMs; CD163+), and tissue-resident memory T cells (CD103+). The presence of these immune markers was evaluated for each core by automated multiplex immunofluorescence staining at the Molecular and Cellular Immunology Core (MCIC) facility, BC Cancer Agency. All antibodies were provided by Biocare Medical (Pacheco, CA, USA) and distributed by Inter Medico (Markham, ON, Canada).

2.4. Automated scoring of multiplex immunofluorescence staining for immune markers

The stained TMA sections were scanned using the Vectra multispectral imaging system. Tissue segmentation into stromal and epithelial compartments was performed using PerkinElmer's (Hopkinton, MA, USA) inForm software. Ten randomly selected cores were utilized to train three independent algorithms in PerkinElmer's inForm software package. The inForm software identified positive pixels for all the selected immune markers using each of the three independent algorithms. The average of the three independent algorithms was taken for all three sets of immune markers in each core. Cores that were missing $\geq$75% of the tissue were excluded from further analyses.

2.5. Manual validation of automated scoring of multiplex immunofluorescence staining

Standard deviation between the three algorithms was calculated for each of the immune markers within both the epithelial and the stromal compartment. Outliers were identified and cross-referenced with the composite image of the corresponding TMA core to verify the discrepancy before excluding the outlying data points from further analysis. Any quantifications that included mis-identification of histological artifacts as immune cells by any of the three algorithms were also excluded from analysis. Algorithms that consistently over- or under-called the immune marker quantification were excluded from analysis. Further visual validation of the automated scoring was performed for randomly selected TMA cores.

2.6. Statistical analysis

Analyses were conducted using R version 3.5.3. Kaplan-Meier curves were plotted using log-rank statistics with survival and survminer packages. Follow-up time for Kaplan-Meier curves ended when 10% of patients remained in each group [21]. Log-rank statistics were used to optimize thresholds for an ideal number of CD163+ M2-like TAMs/CD79a + B cells associated with shorter recurrence-free survival (RFS), using the maxstat package in R. Optimal thresholds are summarized in Supplementary Table 3. Univariate and multivariable analyses were performed and visualized using the survival and ggplot2 packages in R.

3. Results

3.1. Female patients with high-grade NMIBC exhibit shorter PFS

In the KHSC cohort, 22% of the patients were female, 60% of the entire cohort had high-grade disease at original presentation, and the majority (88%) did not have evidence of BCG immunotherapy prior to collection of their specimens (BCG naïve). Approximately 54% of patients received one or more doses of BCG. Clinical care of all patients was coordinated at a single treatment clinic, and decisions regarding adjuvant therapies were based on risk stratification in concordance with American Urological Association (AUA) risk stratification [22]. The UROMOL cohort had a similar proportion of female patients (22%). The proportions of patients who underwent BCG immunotherapy were 19% and 54% in the UROMOL and KHSC cohorts, respectively. In alignment with previous reports on sex-associated differential outcomes, female patients with high-grade NMIBC had shorter PFS than their male counterparts in both the cohorts (Fig. 1A and B).

in the epithelial (left) and stromal (right) compartments of tumors from the KHSC cohort. Plots were stratified by low- and high-grade samples for males (blue) versus females (pink). Significant differences were signified by asterisks between grades (with bracket) and between sexes (no bracket), as determined by the Mann-Whitney *U* test. * $p < 0.05$. ** $p < 0.01$. *** $p < 0.001$. (F) In a subset of patients from the KHSC cohort that recurred in <1 yr, female patients had significantly higher density of CD163+ cells in the stroma and epithelium, while there were no significant sex-associated differences in CD79a+ cells. * $p < 0.05$. (G) Spearman correlation plot for CD163+, CD79a+, and PD-L1+ populations in the epithelial (Epi) and stromal (Str) compartments of tumors from the KHSC cohort. Dark blue indicates a positive correlation coefficient (>1), and dark red indicates a negative correlation coefficient (<1). (H) Violin plots of the mean cell counts for PD-L1+ cell populations in the epithelial (left) and stromal (right) compartments of tumors from the KHSC cohort. Plots were stratified by low- and high-grade samples for males (blue) versus females (pink). Differences between grades in each compartment were determined by the Mann-Whitney *U* test. *** $p < 0.001$. HG = high-grade; KHSC = Kingston Health Sciences Center; LG = low-grade; NMIBC = non–muscle-invasive bladder cancer; PFS = progression-free survival.

3.2. High-grade tumors from female patients with NMIBC exhibit increased expression of immune regulatory genes

Using whole transcriptome profiles of tumors in the UROMOL cohort, a targeted analysis was performed to determine grade- and sex-associated differential expression patterns of genes identifying immune cell phenotypes (specifically macrophages, T cells, and B cells), their functional states, and immune regulatory functions [18]. Significantly higher expression of the immune checkpoint genes *CTLA4*, *PDCD1*, *LAG3*, and *ICOS* were observed in high-grade tumors from females than in those from males and in low-grade tumors from both sexes (Fig. 1C). Importantly, transcript levels of B-cell–recruiting chemokine, *CXC ligand 13* (*CXCL13*), and B-cell surface-associated molecule, *CD40*, were significantly increased in high-grade tumors from female patients (Fig. 1C).

3.3. Tumors from female patients with NMIBC have increased CD163+ M2-like macrophages, CD79a+ B cells, and higher PD-L1 immune checkpoint protein expression

Based on the differences in immunoregulatory gene expression profiles investigated in the UROMOL cohort, we next evaluated sex-associated differences in the density and localization of a subset of immune cells that are known to express the relevant phenotypic markers and immune checkpoint proteins, and have the potential to secrete the cytokine CXCL13. As such, we investigated the epithelial and stromal density profiles of T helper (CD3+CD8–), T cytotoxic (CD8+Ki67– and activated CD8+Ki67+), T regulatory (CD3+CD8– and FOXP3+), T tissue resident memory (CD103+), B cells (CD79a), M2-like TAMs (CD163+), and immune checkpoint proteins (PD-1 and PD-L1) in tumors from the KHSC cohort.

Interestingly, among all the immune cell phenotypes, only CD163+ M2-like TAMs demonstrated statistically significant differences in the density and localization between both low- and high-grade tumors from male and female patients. Significantly higher infiltration of CD163+ TAMs was seen in the epithelial compartment of low-grade tumors ($p = 0.012$) and in both the epithelial and the stromal compartment of high-grade tumors ($p = 0.001$ and $p < 0.001$, respectively) from female patients than in those from male patients (Fig. 1D). Density of CD79a+ B cells was not significantly different between sexes; however, CD79a+ B-cell infiltration was higher in the epithelial and stromal compartments ($p < 0.001$) of high-grade tumors than in those of low-grade tumors from both sexes (Fig. 1E). Importantly, tumors from female patients exhibiting recurrence within 1 yr showed significantly higher density of CD163+ TAMs than those from males (Fig. 1F). With respect to CD79a+ B cells, a trend toward higher infiltration was observed in tumors from female patients who recurred within 1 yr of BCG treatment (Fig. 1F). Spearman correlation analysis showed a moderate positive correlation ($r = 0.63$; $p < 0.0001$) between stromal CD79a+ B cells and CD163+ TAMs (Fig. 1G).

PD-L1 protein expression was significantly higher in both the epithelial and the stromal compartment of high-grade tumors than in low-grade tumors (Fig. 1H; $p < 0.001$). However, apparent sex-associated differences in PD-L1 protein expression (especially in the epithelial compartment) were likely not statistically significant due to the wide variability in the proportion of PD-L1+ cells given its dynamic nature of expression.

A subset analysis of cases was performed in patients who had no evidence of previous intravesical BCG immunotherapy (BCG naïve) by excluding from the entire cohort those patients who had documented BCG prior to specimen collection or for whom that data could not be determined definitively. Trends in infiltration profiles of CD163 and CD79a between grades and between sexes were consistent with those seen in the whole cohort (Supplementary Fig. 2A–C), although in this analysis, expression of PD-L1 protein in the epithelial compartment of low-grade tumors from females was significantly higher than in tumors from males ($p = 0.04$).

3.4. Regulatory T cells and CD3+CD8– T cells exhibit significant sex differences in density and spatial distribution within the NMIBC TIME

While we observed no sex-associated differences in the density and spatial organization of CD8+ cytotoxic T cells, CD3+CD8– T cells and CD3+CD8-FoxP3+ T regulatory cells were significantly higher in low-grade tumors from female patients than in those from male patients (Supplementary Fig. 3A and B). Such differences were not observed in high-grade tumors.

3.5. Increased density of CD163+ M2-like macrophages and CD79a+ B cells associates with early recurrence in NMIBC

Kaplan-Meier analysis for all patients with high-grade NMIBC ($n = 170$) in the KHSC cohort showed that, irrespective of their localization in the stroma or epithelium, higher density (Supplementary Table 2) of CD163+ M2-like TAMs (Fig. 2A) and CD79a+ B cells (Fig. 2B) was independently associated with shorter RFS. This association was observed in both male and female patients, supporting the notion that rather than being a sexually dimorphic epiphenomenon, these cells may play a functional role in tumor recurrence (Fig. 2C and 2D). Notably, these differences in RFS remained consistent using similar thresholds for both CD79a+ and CD163+ cells, in all patients with high-grade tumors (Supplementary Fig. 4A, 4B, 5A, and 5B). Univariate analysis performed for all high-grade patients confirmed that epithelial and stromal CD163+ cell populations and stromal CD79a+ cells were significantly associated with RFS, while age, sex, previous BCG treatment, and induction BCG treatment were not. However, multivariable analysis conducted on all high-grade patients revealed that only AUA Risk Score (hazard ratio [HR] 3.36 [95% confidence interval {CI} ±1.76–6.20]) was significantly associated with RFS. Owing to the potential interaction between risk stratification and intensity of BCG therapy, we further analyzed a subset of high-grade patients who received adequate (≥5) BCG induction ($n = 118$). Univariate analysis

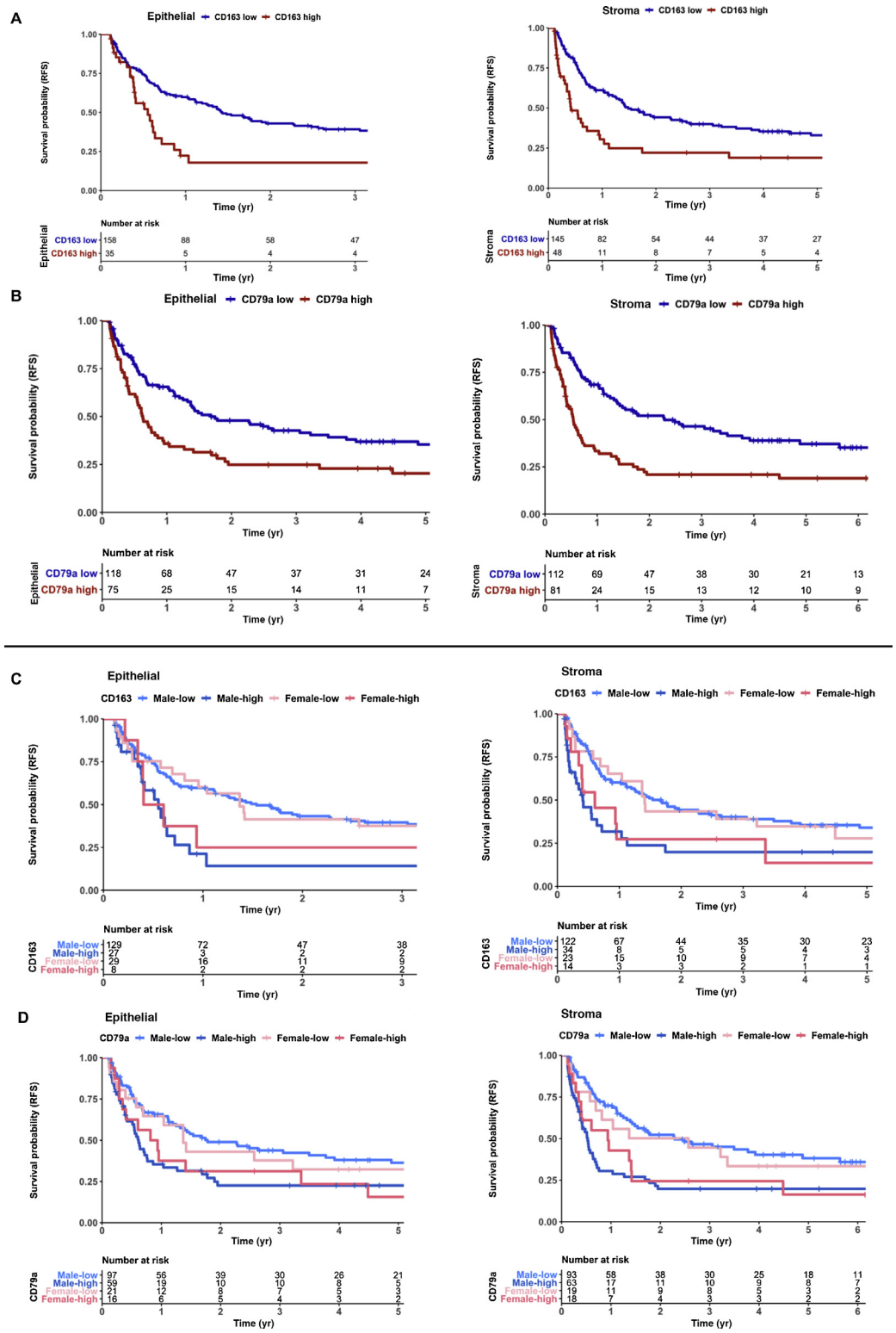

Fig. 2 – Recurrence-free survival (RFS) in high-grade NMIBC is associated with patient sex and tumor immune microenvironment. (A) Kaplan-Meier survival curves for RFS of patients with high-grade NMIBC (n = 193) based on log-rank optimized thresholds for density of CD163+ cells in tumor epithelial (left; $p < 0.001$) and stromal (right; $p < 0.001$) compartments. Of this entire cohort, 74% had evidence of adequate BCG therapy after specimen collection (TURBT). (B) Kaplan-Meier survival curves showing RFS of high-grade patients based on log-rank optimized thresholds for epithelial (left; $p < 0.01$) and stromal (right; $p < 0.0001$) CD79a+ cells. (C) Kaplan-Meier survival curves showing RFS of high-grade patients based on log-rank optimized thresholds for stromal (left; $p < 0.01$) and epithelial (right; $p = 0.014$) CD163+ cells stratified by sex. High and low stromal CD163+ cells are defined as >64 and <64 cells, respectively. High and low epithelial CD163+ cells are defined as >12 and <12 cells, respectively. (D) Kaplan-Meier survival curves showing RFS of high-grade patients based on log-rank optimized thresholds for stromal (left; $p < 0.001$) and epithelial (right; $p = 0.028$) CD79a+ cells stratified by sex. High and low stromal CD79a+ cells are defined as >35 and <35 cells, respectively. High and low epithelial CD79a + cells are defined as more than three and fewer than three cells, respectively. BCG = bacillus Calmette-Guérin; NMIBC = non–muscle-invasive bladder cancer; TURBT = transurethral resection of bladder tumor.

again demonstrated that RFS was significantly associated with AUA Risk Score, epithelial CD163+ cell populations, and both epithelial and stromal CD79a+ cells; however, only AUA Risk Score remained significant upon multivariate analysis (HR 2.40 [95% CI 1.14–5.10]). To further control for the interactions between AUA Risk Score and BCG use, we subset for only AUA high-risk patients with adequate BCG use (n = 94), and the same clinical and TIME variables remained significant for RFS in univariate analysis, although none remained significant upon multivariable analysis potentially due to the small cohort size.

4. Discussion

In the current study, we report the first demonstration of sexual dimorphism in the TIME of NMIBC. In concordance with previous reports [4–6], we found that female patients with high-grade NMIBC suffer from shorter PFS as compared with their male counterparts. An analysis of a panel of immune regulatory genes (both stimulatory and inhibitory) in tumors from the UROMOL cohort demonstrated increased expression of immune checkpoint genes, and those associated with B-cell recruitment and function in high-grade tumors from females compared with those from males. These alterations are indicative of an exhausted immune landscape following increased activation within the NMIBC TIME. Given the dynamic nature of immune checkpoint gene expression, variability in checkpoint coexpression, and an expected lack of direct correlation with protein-level expression, we investigated the profiles of cell types known to express these molecules following activation or exhaustion.

Our finding of higher infiltration of CD163+ M2-like suppressive TAMs in tumors from female patients is of interest and leads us to hypothesize that this finding could partially explain the inferior outcomes experienced by female patients following BCG immunotherapy. A significantly increased density of M2-like TAMs in tumors from female patients may be driven by differences dictated by sexual dimorphism in overall bladder mucosal immune physiology [17]. Indeed, higher infiltration of tumors by CD163+ M2-like TAMs has previously been reported to be associated with poor clinical outcomes in NMIBC [23]. It is also known that bladder cancer cells induce the polarization of tissue-resident and reactive macrophages [24], potentially influencing tumor progression and treatment response [25]. Our novel findings of the higher density of B cells in tumors from female patients are reflective of the established physiological links between M2-like TAMs and B cells [26]; costimulation of M2-like macrophages with bacterial lipopolysaccharide and interleukin (IL)-10 induces production of CXCL13, a chemokine critical for B-cell recruitment [27,28]. Given the increased incidence of urinary tract infections in women—and the cancer cell-induced polarization of TAMs toward an M2-like phenotype [24]—it is plausible that increased engagement of M2-like TAMs by urinary pathogens or cancer cell induced polarization leads to high CXCL13 secretion and B-cell recruitment in tumors of female patients with NMIBC. Eventually, these recruited cells acquire a dysfunctional or exhausted phenotype, persisting in an immunological stalemate within the NMIBC TIME. This observation is further strengthened by our in silico transcriptomic analysis showing increased expression of *CXCL13*; however, further mechanistic evidence is warranted. Similarly, it is also known that IL-10 secreted by B regulatory cells inhibits macrophage activation and polarizes them toward an M2-like phenotype [29]. Furthermore, we also observed significantly increased expression of the immune checkpoint *HAVCR1* (encodes TIM-1) in high-grade tumors from both male and female patients. It is known that *HAVCR1* plays a critical role in IL-10 production by B cells (and potentially T regulatory cells) [30]. However, since bulk RNA-sequencing data do not provide information on the precise source of cell type exhibiting such high expression, future investigations are warranted to identify the cell source within the TIME. Indeed, under normal physiological conditions, females exhibit higher proportions of B cells and increased responsiveness to BCG vaccination [31,32]. However, given the older age of patients with NMIBC, it is possible that a reduced naïve B-cell pool in the periphery [33] compromises the desired responses in the NMIBC scenario following local BCG administration in contrast to responses associated with infant vaccination. We acknowledge that the static TIME states evaluated in this study, however, do not provide definitive evidence supporting these temporal phenomena and warrant further investigation.

A novel finding from our study is the inverse association of B cells and CD163+ M2-like TAMs with RFS in BCG-naïve patients. This finding has significant implications in advancing the current state of knowledge on the antigen-presenting function of these cells following encounter with BCG bacteria upon their intravesical administration. For example, it is known that M2-like macrophages exhibit tolerance and are unable to secrete CXCL10 [34], which limit their ability to recruit immune cells to the TIME. However, BCG treatment has been shown to reprogram M2 macrophages [35] that may lead to some degree of the observed antitumor responses. B cells have been shown to be indicators of good prognosis in certain cancers [36,37]. However, their antitumor roles depending on either their antibody-producing or their antigen presentation function, neither of which are well understood in NMIBC. The negative prognostic association of B cells, as observed in this study, indicates their potentially exhausted or regulatory phenotype. A comprehensive analysis of their functional states is needed to define their tumor killing or promoting roles.

Another important finding from this study is the sex-associated difference in PD-L1 protein expression. PD-L1 is known to be expressed on a wide variety of immune cells and cancer cells, and is partially regulated by estrogen and X-linked microRNAs [38,39]. Indeed, pre-treatment PD-L1 expression was recently shown to be predictive of response to BCG [40]. The finding suggestive of overall higher PD-L1 expression in tumors from females may inform improved use of combination therapies targeting this immune

checkpoint in female patients despite the caveats associated with the dynamic nature of its expression.

Findings from this study could inform immunotherapy trials that are adequately powered to evaluate responses in female patients with NMIBC. Increased abundance of CD163 + M2-like macrophages may also explain the compounding effects of these suppressive factors that impart an aggressive behavior, leading to poor clinical outcomes experienced by female patients relative to males. Several trials targeting CD40 or CSF1R (M2 TAM targeting) in combination with PD-L1 immune checkpoint blockade are underway in a variety of cancers [41], outcomes of which might inform their potential use in NMIBC.

Our study is not without limitations. PD-L1 immune checkpoint is expressed on a wide variety of cells, including cancer and immune cells in the TIME. Future studies evaluating the colocalization of immune checkpoints in tumors from NIMBC patients should derive definitive information on cell types expressing this immune checkpoint. Furthermore, a more comprehensive evaluation of the functional states of immune cells and immunogenomic correlates driving their recruitment via cell intrinsic interferon activation is needed to guide more precise therapeutic targeting. Finally, the single-institution KHSC cohort size was insufficient to investigate any independent association of the TIME findings and recurrence in multivariable analysis, but it provides rationale for future, large multi-institutional studies to validate the sexual dimorphism observations that we have identified in NMIBC and their clinical relevance.

5. Conclusions

Findings from study highlight the importance of patient sex in evaluating response to immunomodulatory therapies in NMIBC and may have significant implications in ongoing immune checkpoint blockade trials where sex-associated pretreatment tumor immune landscape could inform their precise use in drug sequencing.

***Author contributions*:** Madhuri Koti had full access to all the data in the study and takes responsibility for the integrity of the data and the accuracy of the data analysis.

Study concept and design: Koti, Siemens.
Acquisition of data: Chenard, Jackson, Vidotto.
Analysis and interpretation of data: Chenard, Jackson, Vidotto, Koti, Siemens.
Drafting of the manuscript: Chenard, Jackson, Koti.
Critical revision of the manuscript for important intellectual content: Chenard, Jackson, Vidotto, Chen, Hardy, Jamaspishvilli, Berman, Siemens, Koti.
Statistical analysis: Vidotto, Jackson.
Obtaining funding: Koti, Siemens, Berman.
Administrative, technical, or material support: Koti, Siemens, Chen, Berman, Jackson.
Supervision: Koti, Siemens, Berman.
Other: None.

***Financial disclosures*:** Madhuri Koti certifies that all conflicts of interest, including specific financial interests and relationships and affiliations relevant to the subject matter or materials discussed in the manuscript (eg, employment/affiliation, grants or funding, consultancies, honoraria, stock ownership or options, expert testimony, royalties, or patents filed, received, or pending), are the following: None.

***Funding/Support and role of the sponsor*:** This work is supported by the Early Researcher Award, Ontario Ministry of Research Innovation and Science, and the Mary and Mihran Basmajian award for Excellence in Health Research, Queen's University, to Madhuri Koti, and SEAMO Innovation award to D. Robert Siemens and Madhuri Koti. Support for sample acquistion and cohort assembly was provided by the Ontario Institute for Cancer Research through funding provided by the Government of Ontario. The Cancer Research Society and Bladder Cancer Canada through the Operating Grant Funding Program to D. M. Berman. Fellowship support for S. Chenard was provided by the Franklin Bracken Fellowship, Queen's University. C. Jackson was supported through the R.J Wilson Fellowship and R. Samuel McLaughlin Fellowship, Queen's University.

***Acknowledgments*:** Katy Milne at BC Cancer's Molecular and Cellular Immunology Core Histology Department at the Trev and Joyce Deeley Research Centre helped with the antibody panel design and multiplex immunofluorescence staining and imaging. We thank Dr. Lars Dyrsjkjot (Aarhus University, Denmark) for sharing RNA-sequencing profiles from the UROMOL NMIBC cohort. UROMOL study tumor transcriptome profiles were accessed from Hedegaard et al [18] with permission, and archival formalin-fixed tissue patient specimens were obtained from Kingston Health Sciences Center.

Appendix A. Supplementary data

Supplementary material related to this article can be found, in the online version, at doi:https://doi.org/10.1016/j.euros.2021.05.002.

References

[1] Bray F, Ferlay J, Soerjomataram I, Siegel RL, Torre LA, Jemal A. Global cancer statistics 2018: GLOBOCAN estimates of incidence and mortality worldwide for 36 cancers in 185 countries. CA Cancer J Clin 2018;68:394–424.
[2] Woldu SL, Bagrodia A, Lotan Y. Guideline of guidelines: non-muscle-invasive bladder cancer. BJU Int 2017;119:371–80.
[3] Sylvester RJ, van der Meijden APM, Oosterlinck W, et al. Predicting recurrence and progression in individual patients with stage Ta T1 bladder cancer using EORTC risk tables: a combined analysis of 2596 patients from seven EORTC trials. Eur Urol 2006;49:466–7.
[4] Kluth LA, Fajkovic H, Xylinas E, et al. Female gender is associated with higher risk of disease recurrence in patients with primary T1 high-grade urothelial carcinoma of the bladder. World J Urol 2013;31:1029–36.
[5] Marks P, Soave A, Shariat SF, Fajkovic H, Fisch M, Rink M. Female with bladder cancer: what and why is there a difference? Transl Androl Urol 2016;5:668–82.
[6] Uhlig A, Strauss A, Seif Amir Hosseini A, et al. Gender-specific differences in recurrence of non-muscle-invasive bladder cancer: a systematic review and meta-analysis. Eur Urol Focus 2018;4:924–36.
[7] Conforti F, Pala L, Bagnardi V, et al. Cancer immunotherapy efficacy and patients' sex: a systematic review and meta-analysis. Lancet Oncol 2018;19:737–46.
[8] Wang C, Qiao W, Jiang Y, et al. Effect of sex on the efficacy of patients receiving immune checkpoint inhibitors in advanced non-small cell lung cancer. Cancer Med 2019;8:4023–31.

[9] Wu Y, Ju Q, Jia K, et al. Correlation between sex and efficacy of immune checkpoint inhibitors (PD-1 and CTLA-4 inhibitors). Int J Cancer 2018;143:45–51.
[10] Saginala K, Barsouk A, Aluru JS, Rawla P, Padala SA, Barsouk A. Epidemiology of bladder cancer. Med Sci (Basel) 2020;8:15.
[11] Koti M, Ingersoll MA, Gupta S, et al. Sex differences in bladder cancer immunobiology and outcomes: a collaborative review with implications for treatment. Eur Urol Oncol 2020;3:622–30.
[12] Binnewies M, Roberts EW, Kersten K, et al. Understanding the tumor immune microenvironment (TIME) for effective therapy. Nat Med 2018;24:541–50.
[13] Annels NE, Simpson GR, Pandha H. Modifying the non-muscle invasive bladder cancer immune microenvironment for optimal therapeutic response. Front Oncol 2020;10:175.
[14] Roumiguié M, Compérat E, Chaltiel L, et al. PD-L1 expression and pattern of immune cells in pre-treatment specimens are associated with disease-free survival for HR-NMIBC undergoing BCG treatment. World J Urol. July 14. https://doi.org/10.1007/s00345-020-03329-2.
[15] Giraldo NA, Sanchez-Salas R, Peske JD, et al. The clinical role of the TME in solid cancer. Br J Cancer 2019;120:45–53.
[16] Mora-Bau G, Platt AM, van Rooijen N, Randolph GJ, Albert ML, Ingersoll MA. Macrophages subvert adaptive immunity to urinary tract infection. PLoS Pathog 2015;11:e1005044.
[17] Zychlinsky Scharff A, Rousseau M, Lacerda Mariano L, et al. Sex differences in IL-17 contribute to chronicity in male versus female urinary tract infection. JCI insight 2019;5:e122998.
[18] Hedegaard J, Lamy P, Nordentoft I, et al. Comprehensive transcriptional analysis of early-stage urothelial carcinoma. Cancer Cell 2016;30:27–42.
[19] Humphrey PA, Moch H, Cubilla AL, Ulbright TM, Reuter VE. The 2016 WHO classification of tumours of the urinary system and male genital organs—part B: prostate and bladder tumours. Eur Urol 2016;70:106–19.
[20] Vidotto T, Nersesian S, Graham C, Siemens DR, Koti M. DNA damage repair gene mutations and their association with tumor immune regulatory gene expression in muscle invasive bladder cancer subtypes. J Immunother Cancer 2019;7:148.
[21] Pocock SJ, Clayton TC, Altman DG. Survival plots of time-to-event outcomes in clinical trials: good practice and pitfalls. Lancet (Lond) 2002;359:1686–9.
[22] Matulewicz RS, Steinberg GD. Non-muscle-invasive bladder cancer: overview and contemporary treatment landscape of neoadjuvant chemoablative therapies. Rev Urol 2020;22:43–51.
[23] Wu S-Q, Xu R, Li X-F, Zhao X-K, Qian B-Z. Prognostic roles of tumor associated macrophages in bladder cancer: a system review and meta-analysis. Oncotarget 2018;9:25294–303.
[24] Martínez VG, Rubio C, Martínez-Fernández M, et al. BMP4 induces M2 macrophage polarization and favors tumor progression in bladder cancer. Clin Cancer Res 2017;23:7388–99.
[25] Suriano F, Santini D, Perrone G, et al. Tumor associated macrophages polarization dictates the efficacy of BCG instillation in non-muscle invasive urothelial bladder cancer. J Exp Clin Cancer Res 2013;32:87.
[26] Mantovani A. B cells and macrophages in cancer: yin and yang. Nat Med 2011;17:285–6.
[27] Mantovani A, Sica A, Sozzani S, Allavena P, Vecchi A, Locati M. The chemokine system in diverse forms of macrophage activation and polarization. Trends Immunol 2004;25:677–86.
[28] Vidyarthi A, Agnihotri T, Khan N, et al. Predominance of M2 macrophages in gliomas leads to the suppression of local and systemic immunity. Cancer Immunol Immunother 2019;68:1995–2004.
[29] Fehres CM, van Uden NO, Yeremenko NG, et al. APRIL induces a novel subset of IgA(+) regulatory B cells that suppress inflammation via expression of IL-10 and PD-L1. Front Immunol 2019;10:1368.
[30] Xiao S, Brooks CR, Zhu C, et al. Defect in regulatory B-cell function and development of systemic autoimmunity in T-cell Ig mucin 1 (Tim-1) mucin domain-mutant mice. Proc Natl Acad Sci U S A 2012;109:12105–10.
[31] Birk NM, Nissen TN, Kjærgaard J, et al. Effects of bacillus Calmette-Guérin (BCG) vaccination at birth on T and B lymphocyte subsets: results from a clinical randomized trial. Sci Rep 2017;7:12398.
[32] Fink AL, Engle K, Ursin RL, Tang W-Y, Klein SL. Biological sex affects vaccine efficacy and protection against influenza in mice. Proc Natl Acad Sci U S A 2018;115:12477–82.
[33] Márquez EJ, Chung C-H, Marches R, et al. Sexual-dimorphism in human immune system aging. Nat Commun 2020;11:751.
[34] Porta C, Rimoldi M, Raes G, et al. Tolerance and M2 (alternative) macrophage polarization are related processes orchestrated by p50 nuclear factor kappaB. Proc Natl Acad Sci U S A 2009;106:14978–83.
[35] Lardone RD, Chan AA, Lee AF, et al. *Mycobacterium bovis* bacillus Calmette-Guérin alters melanoma microenvironment favoring antitumor T cell responses and improving M2 macrophage function. Front Immunol 2017;8:965.
[36] Kroeger DR, Milne K, Nelson BH. Tumor-Infiltrating plasma cells are associated with tertiary lymphoid structures, cytolytic T-cell responses, and superior prognosis in ovarian cancer. Clin Cancer Res 2016;22:3005–15.
[37] Wieland A, Patel MR, Cardenas MA, et al. Defining HPV-specific B cell responses in patients with head and neck cancer. Nature. In press. https://doi.org/10.1038/s41586-020-2931-3.
[38] Carè A, Bellenghi M, Matarrese P, Gabriele L, Salvioli S, Malorni W. Sex disparity in cancer: roles of microRNAs and related functional players. Cell Death Differentiation 2018;25:477–85.
[39] Shen Z, Rodriguez-Garcia M, Patel MV, Barr FD, Wira CR. Menopausal status influences the expression of programmed death (PD)-1 and its ligand PD-L1 on immune cells from the human female reproductive tract. Am J Reprod Immunol 2016;76:118–25.
[40] Kates M, Matoso A, Choi W, et al. Adaptive immune resistance to intravesical BCG in non-muscle invasive bladder cancer: implications for prospective BCG-unresponsive trials. Clin Cancer Res 2020;26:882–91.
[41] DeNardo DG, Ruffell B. Macrophages as regulators of tumour immunity and immunotherapy. Nat Rev Immunol 2019;19:369–82.

Supplementary Table 1: Patient characteristics for cohort (n = 332)

Age at Diagnosis	Mean	71.18
	Median	72
	Range	34-94
Sex	Male	259
	Female	73
Initial Diagnosis, Stage and Grade	Ta, Low Grade	134
	Ta, High Grade	120
	T1, High Grade	78
Previous BCG	Yes	25
	No	292
	Unknown	15
BCG	Yes	180
	No	137
	Unknown	15
AUA Risk Score	Low	94
	Intermediate	72
	High	166
Progression to T2	Yes	36
	No	273
	Unknown	23
Recurrence	< 1 year	123
	>1 year	72
	Never	137
Median Follow-up		56.2 months (4.7 years)

Supplementary Table 3: Optimized log-rank thresholds for recurrence-free survival for individual immune markers

	All high-grade patients	**High grade patients recurring within one year**
CD163-Stroma	64	65

CD163-Epithelial	13	N.S
CD79-Stroma	35	N.S
CD79-Epithelial	3	N.S

N.S- No significant differences in recurrence-free survival found for any cut-off

Supplementary Table 2: Sample characteristics for cohort (n = 509)

Stage and Grade	Ta, Low Grade	188
	Ta, High Grade	165
	T1, High Grade	156
Sex	Male	405
	Female	104
CIS	Yes	77
	No	432

Supplementary Figures

Supplementary Figure 1. Multiplex immunofluorescence staining and automated tissue segmentation of representative tumor core. A composite view of a representative tumor core, highlighting antibody panels distinguishing CD3+CD8+Ki67+/- and CD3+CD8-FoxP3- cells (A); CD79a+ B, CD103+ T resident and CD163+ M2-like TAMs (B); PD-1+, PD-L1+ and CK5+ cells (C). PerkinElmer's Inform software based automated segmentation of tumor core into epithelial (red) and stromal (green) compartments prior to automated scoring of positively stained cells (D).

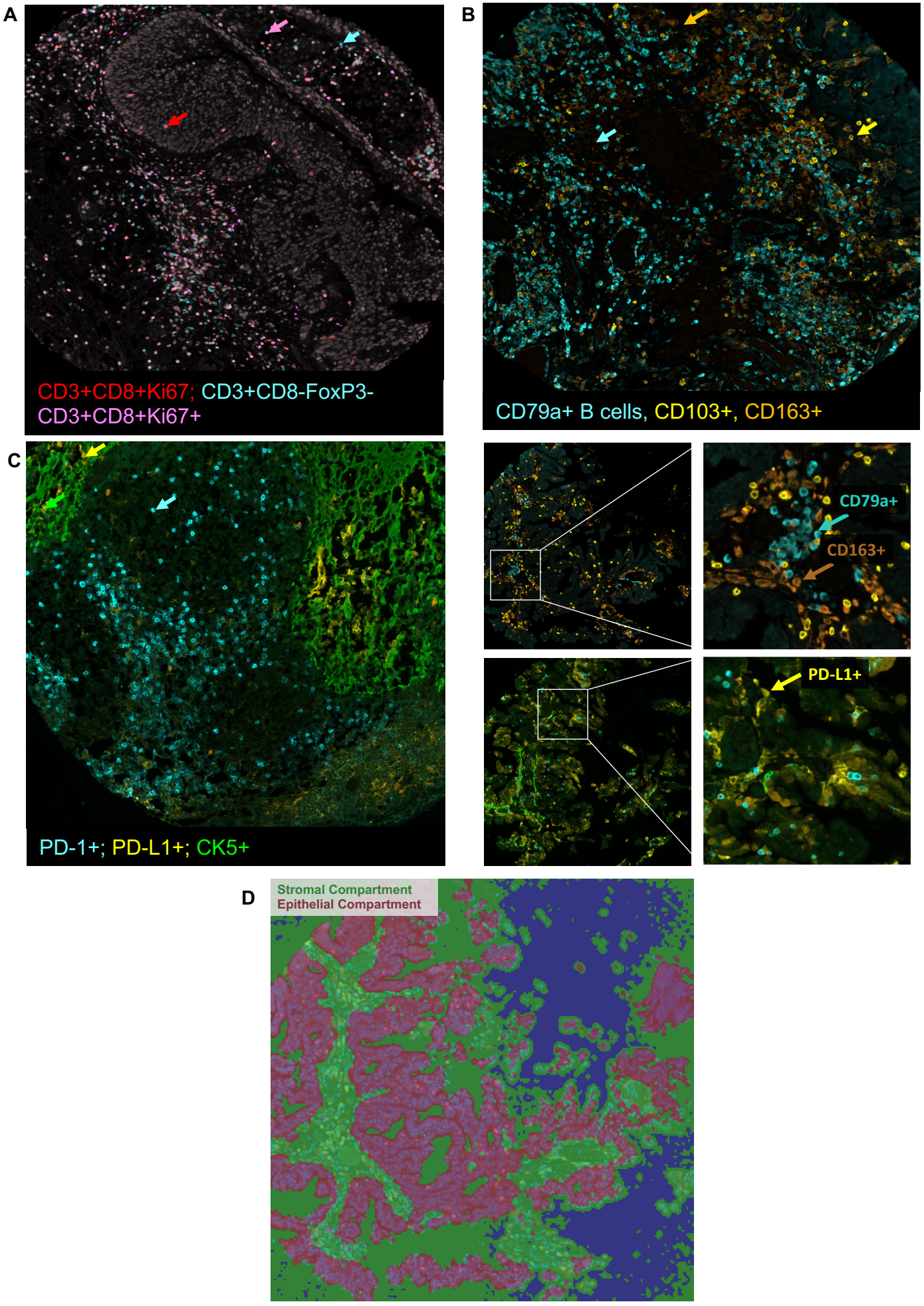

Supplementary Figure 1. Multiplex immunofluorescence staining and automated tissue segmentation of representative tumor core.

Supplementary Figure 2. Profiles of CD163, CD79a and PD-L1 in tumors from BCG naïve patients

Violin plots of mean cell counts for CD163+ (A), CD79a+ (B) and PD-L1+ cell (C) populations respectively, in the epithelial (left) and stromal (right) compartments of tumors from the KHSC cohort with no evidence of BCG immunotherapy prior to collection of their specimens (BCG naïve). Asterisks indicate level of significance as determined by Mann-Whitney-U statistics: ***p-value < 0.001 **p-value < 0.01 *p-value < 0.05.

2A

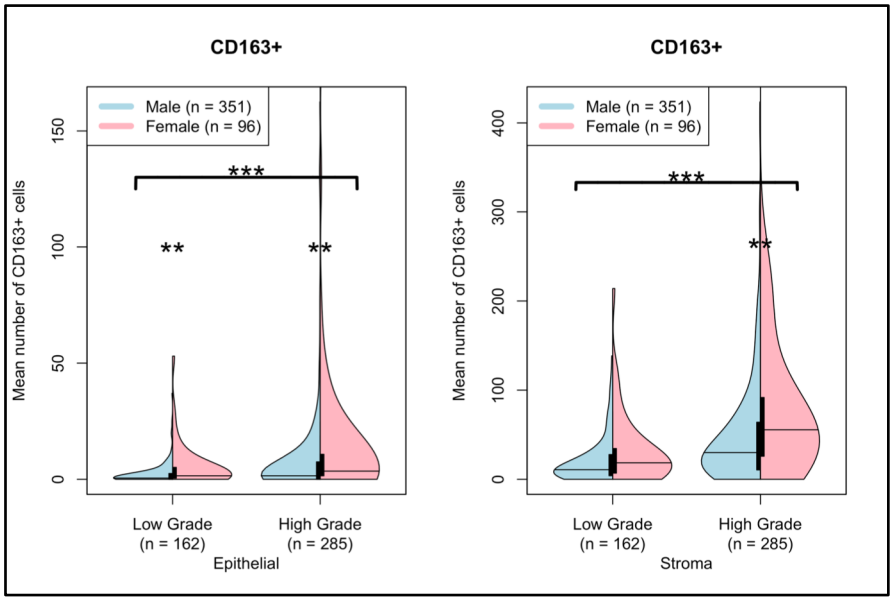

2B

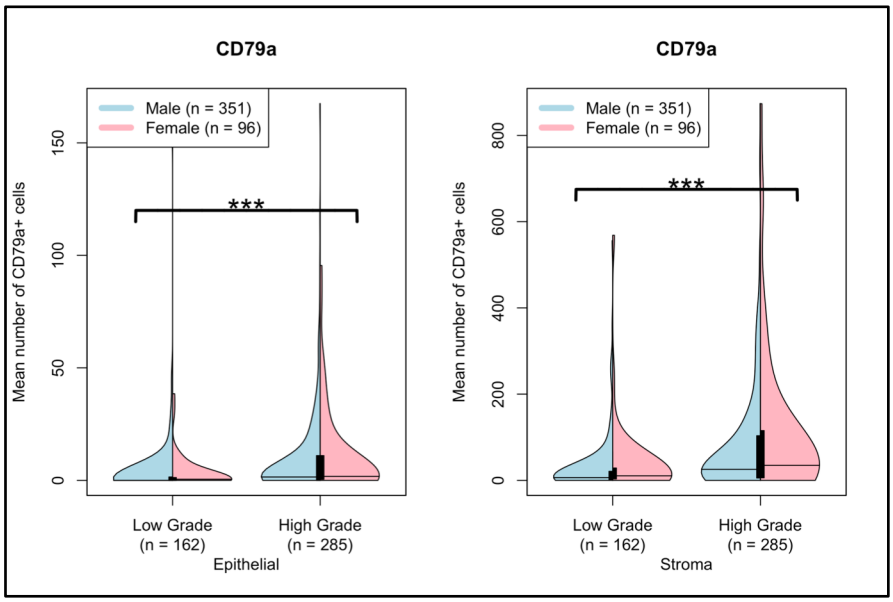

2C

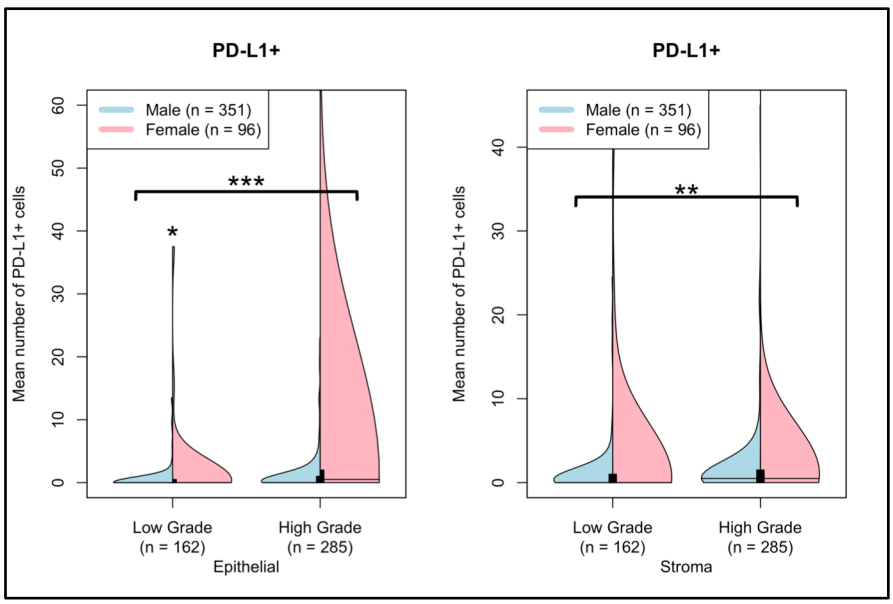

Supplementary Figure 2: Profiles of CD163, CD79a and PD-L1 in tumors from BCG naïve patients

Supplementary Figure 3. Profiles of CD3+CD8-T cells (3A) and regulatory T cells (3B) in tumors from BCG naïve patients and overall cohort

Violin plots of mean cell counts for CD3+CD8- T(A) and CD3+CD8-FoxP3+ T regulatory cells (B) in BCG naïve and overall cohort. Plots stratified by low-grade and high-grade samples for males (blue) versus females (pink). Asterisks indicate level of significance as determined by Mann-Whitney-U statistics: ***p-value < 0.001 **p-value < 0.01 *p-value < 0.05.

3A

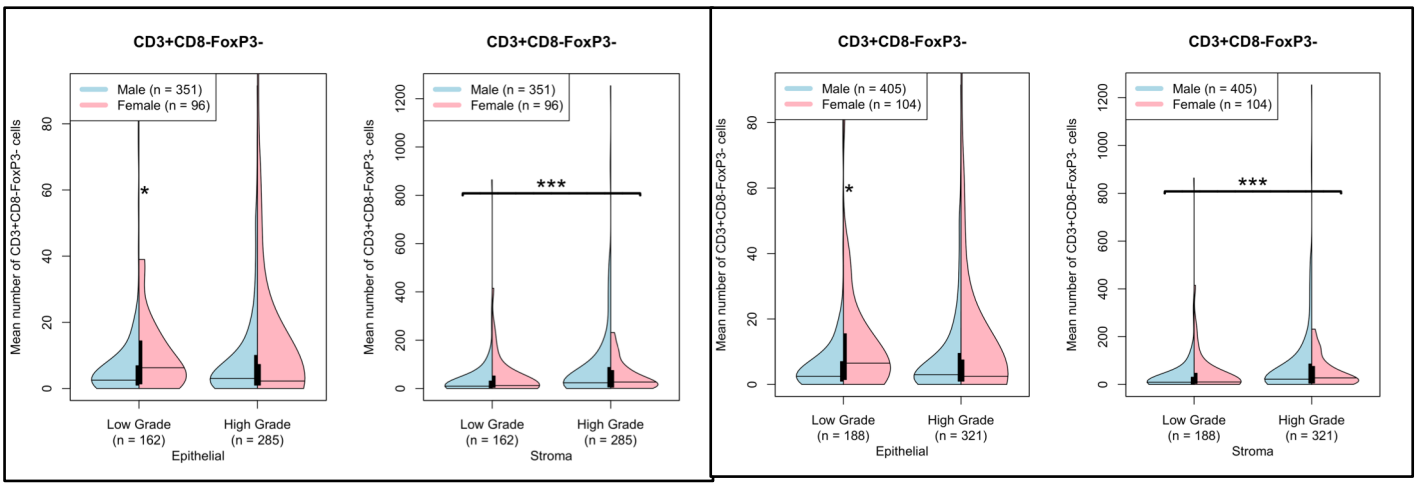

BCG naïve tumors

Overall cohort

3B

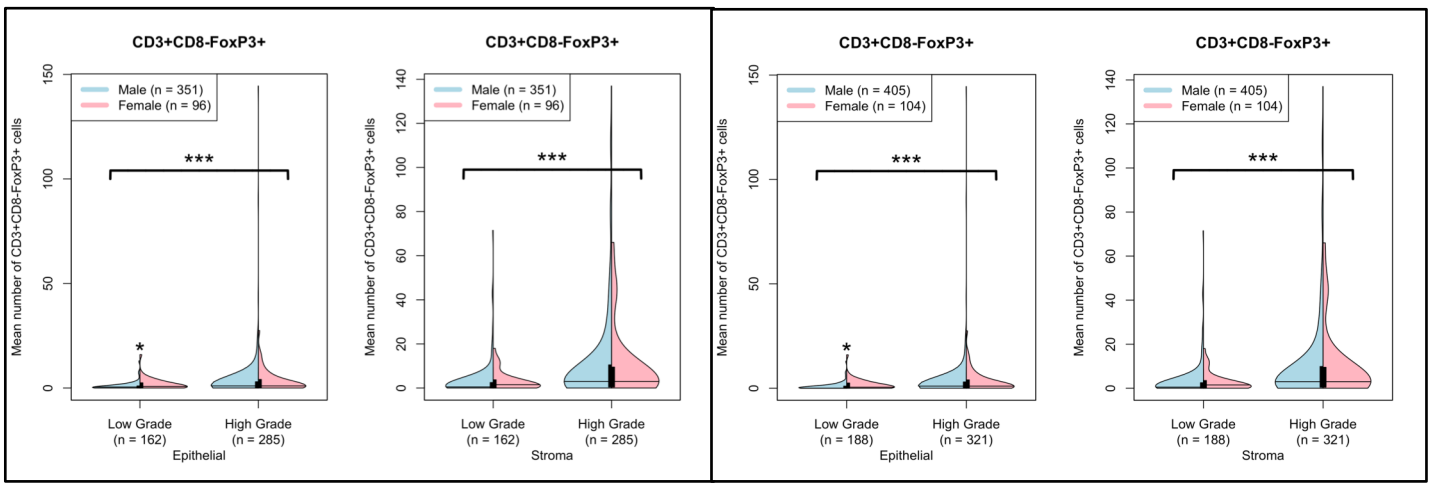

BCG naïve tumors

Overall cohort

Supplementary Figure 3: Profiles of CD3+CD8- T (3A) and regulatory T cells (3B) in tumors from BCG naïve patients and overall cohort

Supplementary Figure 4. CD79a+ B cell density is associated with recurrence free survival in patients with high-grade NMIBC and no prior history of BCG before specimen collection (BCG naïve).

(a) Recurrence-free survival of a subset of patients with high-grade disease and no previous BCG therapy prior to specimen collection (n=170). Within this cohort 74% had evidence of adequate BCG therapy after specimen collection (TURBT). Based on log-rank optimized cut-offs for stromal (left; $p<0.001$) and epithelial (right; $p<0.056$) CD79a+ cells stratified by males (blue) versus females (pink).

(b) Recurrence-free survival based on log-rank optimized cut-offs for stromal (left) and epithelial (right) CD79a+ cells stratified by high CD79a+ cells versus low CD79a+ cells. High versus low stromal CD79a+ cells defined as > 35 or < 35 cells, respectively. High vs low epithelial CD79a+ cells defined as > 3 or < 3 cells, respectively. Associated p-values for the epithelial and stromal compartments is <0.01 and <0.0001, respectively.

Supplementary Figure 5. Higher CD163+ cell infiltration is associated with shorter recurrence free survival in BCG-naïve patients with high-grade NMIBC.

(a) Recurrence-free survival of high-grade, BCG naïve patients (n=170) based on log-rank optimized cut-offs for stromal (left; P=0.017) and epithelial (right; 0.057) CD7163+ cells stratified by males (blue) versus females (pink).

(b) Recurrence-free survival based on log-rank optimized cut-offs for stromal (left) and epithelial (right) CD163+ cells stratified by high CD163+ cells versus low CD163+ cells. High versus low stromal CD163+ cells defined as > 64 or < 64 cells, respectively. High vs low epithelial CD163+ cells defined as > 12 or < 12 cells, respectively. Associated p-values for the epithelial (right) and stromal (left) compartments are both $p<0.01$.

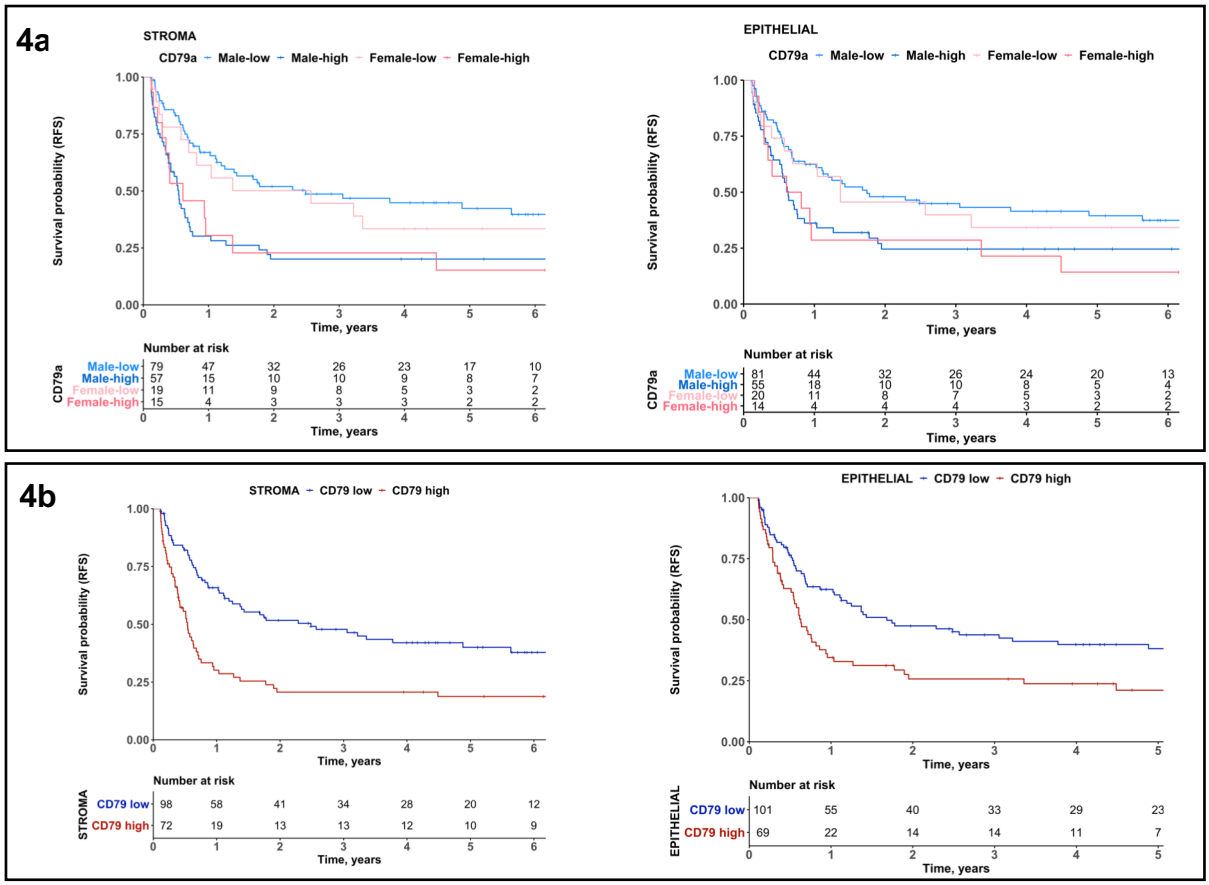

Supplementary Figure 4. CD79a+ B cell density is associated with recurrence free survival in patients with high-grade NMIBC

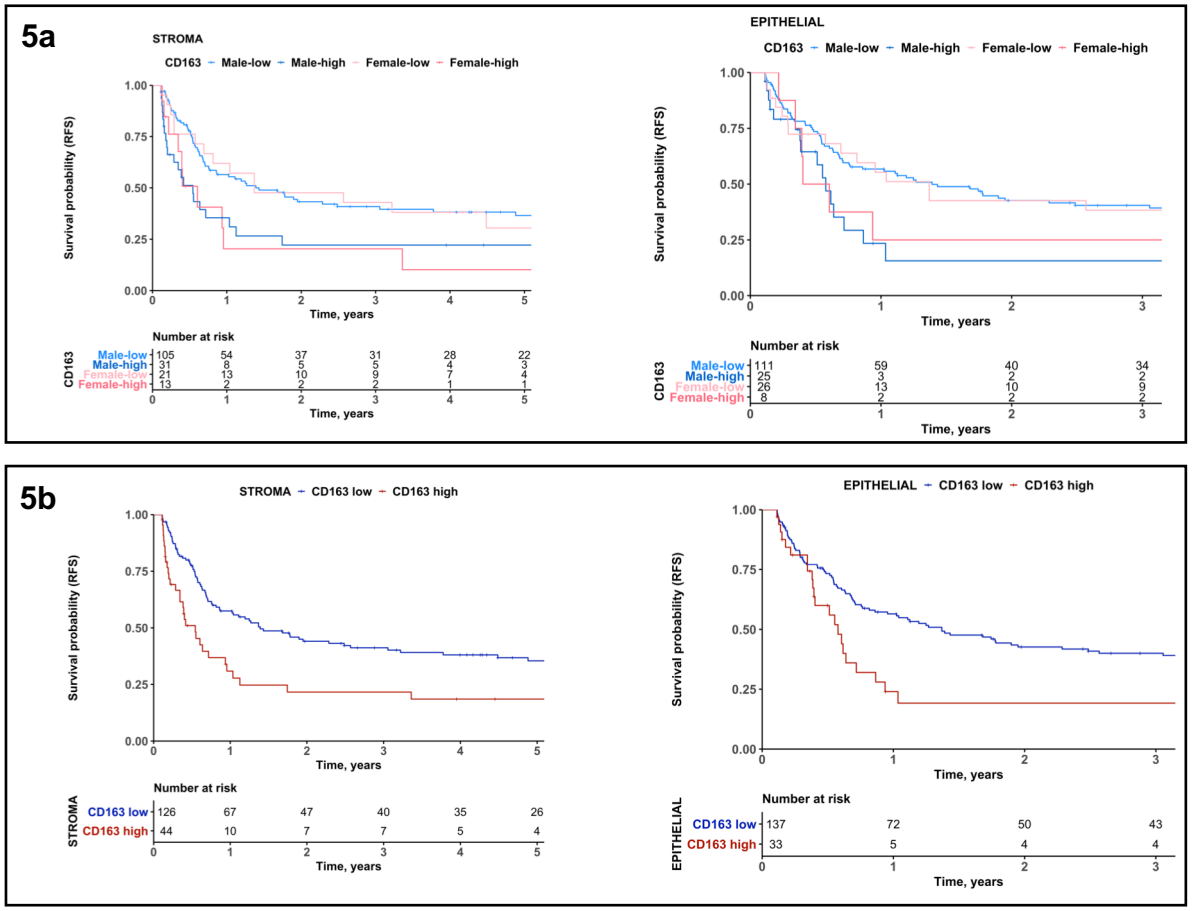

Supplementary Figure 5. Higher CD163+ cell infiltration is associated with shorter recurrence free survival in patients with high-grade NMIBC

Supplementary Figure 6. AUA Risk Score is associated with increased risk of recurrence for patients with high-grade NMIBC who received adequate induction BCG therapy.

(a) Forest plot of multivariate analysis examining the relationship between potential risk factors (age, sex, previous BCG, induction BCG, CD163, CD79a and AUA risk score) and recurrence-free survival for all patients with high-grade NMIBC who received adequate induction BCG therapy (>5 doses) in the KHSC cohort (n=118). Patients with high AUA risk score were 2.40 times more likely to suffer disease recurrence than patients with intermediate AUA risk score (95% CI, 1.14-5.0; $p<0.021$). No other risk factors were found to be significantly associated with RFS ($p>0.05$).

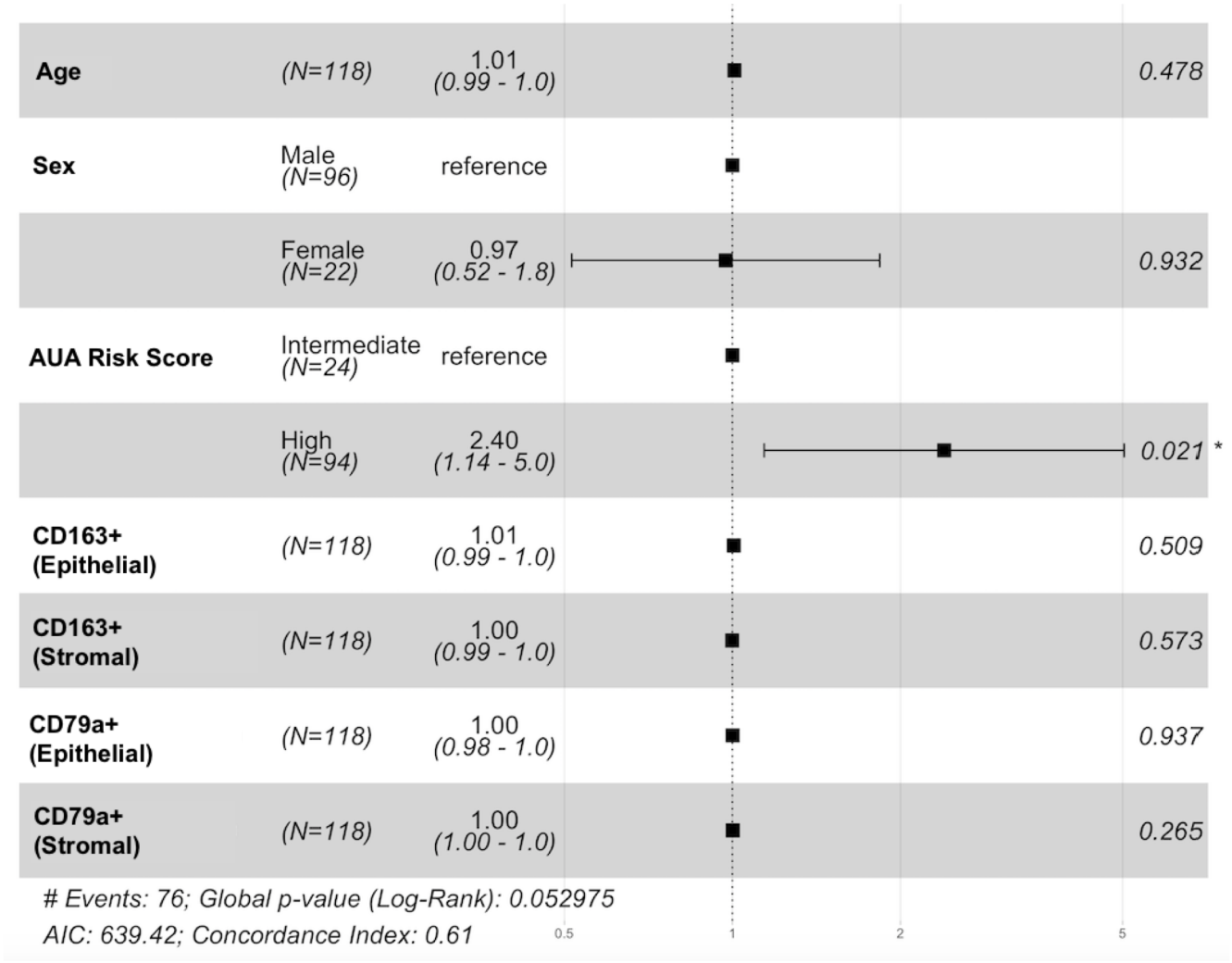

Supplementary Figure 6. AUA Risk Score is associated with increased risk of recurrence for patients with high-grade NMIBC who received adequate induction BCG therapy.

Supplementary Tables

S1. Clinical characteristics of patients in the KHSC cohort (n=332).

S2. Sample characteristics (grade, stage and sex) for overall KHSC cohort (n = 509)

S3. Optimized log-rank thresholds for recurrence-free survival for individual immune markers